Rashi Chaudhary, 2025, 13:4
ISSN (Online): 2348-4098
ISSN (Print): 2395-4752

International Journal of Science, Engineering and Technology

An Open Access Journal

Antibacterial Efficacy of Cufe2o4-Ag@PANI Nanocomposite on Gram- Positive and Gram-Negative Bacteria

Rashi Chaudhary, Garima Nagpal

Department of Life Science, Sharda University, Greater Noida, India
Department of Physics & Environmental Science, Sharda University, Greater Noida, India.

Abstract- This study reports the green synthesis of a $CuFe_2O_4$-Ag@PANI nanocomposite using floral extract as a natural reducing and stabilizing agent, offering an eco-friendly alternative to conventional chemical synthesis. The structural, morphological, and compositional features of the synthesized nanocomposite were thoroughly characterized using FTIR, XRD, FESEM, TEM, and EDX techniques, confirming the formation of well-dispersed, crystalline nanoparticles with spherical morphology and an average size of ~20 nm. Antibacterial efficacy was assessed against Staphylococcus aureus and Escherichia coli through zone of inhibition, minimum inhibitory concentration (MIC), and bacteriostatic rate analysis. The nanocomposite exhibited superior antibacterial activity compared to bare $CuFe_2O_4$, with inhibition zones of 27 mm for S. aureus and 24 mm for E. coli, and MIC values of 62.5 µg/mL and 75 µg/mL, respectively. Bacteriostatic rate analysis showed enhanced bacterial growth inhibition (60.9% for E. coli and 50.5% for S. aureus), confirming the synergistic role of Ag and PANI in improving bactericidal performance. The proposed mechanism involves reactive oxygen species (ROS) generation and membrane disruption. These findings highlight the potential of $CuFe_2O_4$-Ag@PANI as a sustainable and effective antibacterial agent for biomedical and environmental applications.

Keywords- green synthesis, $CuFe_2O_4$-Ag@PANI Nanocomposite, gram- positive bacteria, Gram-Negative bacteria, ROS mechanism.

I. INTRODUCTION

Nanotechnology has revolutionized materials science, particularly by the synthesis of metal-based nanocomposites with enhanced antimicrobial efficacy [1]. Among ferrite materials, with suitable permeability and noticeable resistivity are one of the most useful classes. Spinel ferrites as soft magnetic materials can be employed in the fields of medical, environmental and several other fields. Spinel ferrites such as $CuFe_2O_4$ have attracted tremendous attention due to their reversible physicochemical properties, thereby useful in diverse biomedical and environmental applications [2]. The application of toxic reagents and harsh conditions in traditional methods has compelled researchers to follow green chemistry-based eco-friendly pathways [3]. Since green synthesis is sustainable, biocompatible, and less toxic to the environment, it has become a preferred approach among many researchers for the synthesis of green nanomaterials. Conventional means of synthesis involve high energy input and toxic chemicals, whereas the bio reduction and stabilization of nanoparticles in green synthesis depends on the use of phytochemicals, which are bioactive compounds found in plant extracts [4]. Such

phytochemicals, including flavonoids, tannins, alkaloids, and polyphenols, serve as natural reducing agents, converting metal ions into stable nanoparticles without the use of hazardous chemicals.In the present study, a flower extract has been employed for the environmentally friendly synthesis of the $CuFe_2O_4$-Ag@PANI nanocomposite, while avoiding toxic chemicals that could greatly diminish the environmental footprint of nanomaterial synthesis. The utilization of flower extracts is especially favorable due to their rich phytoconstituents, low-cost nature, and easy accessibility. The biological synthesis guarantees the stability and controlled morphology of the nanoparticles, which are prerequisite parameters for achieving the desired structural and functional properties.

Multiple studies stressed that silver and ferrite-based nanocomposites have greatly improved antimicrobial activity because of their ability to create reactive oxygen species (ROS) or induce membrane disorganization in microbial cells [5]. In fact, ROS mechanisms include the generation of very reactive molecules like superoxide anions (O_2^-), hydroxyl radicals (•OH), and hydrogen peroxide which can attack cellular components such as proteins, DNA, and lipids and finally lead into the oxidative stress of and killing effect to cell death. In addition, the membrane destruction mechanism is aided by the positive charge of the newly formed nanocomposite toward the negatively charged surface of the bacterial cell membrane, resulting in structural damage increased permeability, and complete lysis. The synergism of copper ferrite ($CuFe_2O_4$), silver (Ag) and PANI within the nanocomposite significantly augments the antimicrobial spectrum of action against a wider variety of microbes.

This study adds to developing sustainable nanotechnology by demonstrating the green synthesis of $CuFe_2O_4$-Ag@PANI nanocomposites from flower extracts, which eliminates harmful chemicals and improves antimicrobial performance via ROS generation as well as membrane disruption [4-5]. The results offered could have promising applications in the medical, environmental, and industrial sectors, especially in developing antibacterial coatings, water purification systems, and biomedical devices.

Materials and Experimental

Bacterial Strains

This study used 2 pathogenic S. aureus ATCC 25923 and Escherichia coli strains. The strains were identified through standard biochemical and molecular assays. Subsequently, their susceptibility to ciprofloxacin was assessed using the disk diffusion method by CLSI guidelines [6].

Preparation of Flower Extract

For the Preparation of flower extract, approximately 8 g of floral waste was collected from nearby temples, washed thoroughly with water, dried, and heated in 100 mL of distilled water at 60 °C for 10 minutes. After filtration, the resulting aqueous floral extract was synthesized [7].

Synthesis of $CuFe_2O_4$-Ag@PANI Nanocomposite

To synthesize the $CuFe_2O_4$–Ag@PANI nanocomposite, 0.85 g of $CuCl_2$•$2H_2O$ and 2.7 g of $FeCl_3$•$6H_2O$ (molar ratio 1:2) were dissolved in 100 mL of distilled water and stirred at 80 °C for 60 minutes. A 6 M NaOH solution was then added dropwise to adjust the pH to 12, and the mixture was stirred at 100 °C for another 60 minutes, forming a brownish $CuFe_2O_4$ precipitate. The precipitate was collected by centrifugation, washed thoroughly with distilled water and ethanol, and dried at 100 °C for 60 minutes.

For Ag deposition, 50 mg of the $CuFe_2O_4$ nanocomposite was redispersed in 100 mL of distilled water, followed by the addition of 20 mg of $AgNO_3$. After 45 minutes of sonication, 10 mL of floral waste extract (as a green reducing agent) was added. The solution was stirred at room temperature for 24 hours, facilitating the in-situ green reduction of Ag^+ ions onto the $CuFe_2O_4$ surface. The $CuFe_2O_4$@Ag nanocomposite was then isolated by centrifugation at 12,000 rpm for 20 minutes and dried in a vacuum oven at 80 °C for 8 hours. For polyaniline coating, the dried $CuFe_2O_4$@Ag composite was then dispersed in 100 mL of 1 M HCl, followed by the addition of 0.1 M

freshly distilled aniline monomer under constant stirring. To initiate polymerization, 0.1 M ammonium persulfate (APS) solution was added dropwise at 0–5 °C under continuous stirring for 6 hours. The mixture turned greenish, indicating the formation of polyaniline. The final $CuFe_2O_4$–Ag@PANI nanocomposite was separated by centrifugation, washed with distilled water and ethanol several times and dried under vacuum at 60 °C overnight [8].

Characterization of Synthesized $CuFe_2O_4$-Ag@PANI Nanocomposite

The synthesized $CuFe_2O_4$-Ag@PANI nanocomposite was characterized using various techniques, including Fourier Transform Infrared (FTIR) spectroscopy (Thermo Nicolet 380, USA) with a diffuse reflectance attachment in the range of 400 to 4000 cm^{-1}, X-ray Diffraction (XRD) (Philips X'Pert MPD, Netherlands), Energy Dispersive X-ray Mapping Analysis (EDX-map) (TESCAN MIRA3, Czech Republic), High-Resolution Transmission Electron Microscopy (HRTEM) (JEM 2100F, JEOL, Japan), and Field Emission Scanning Electron Microscopy (FESEM) (TESCAN MIRA3, Czech Republic).

Antibacterial Activity Assay

The antibacterial activity of the $CuFe_2O_4$-Ag@PANI nanocomposite, both alone and in combination with ciprofloxacin, against S. aureus and E. coli was evaluated using the disk diffusion method. Bacterial suspensions were prepared from fresh cultures, adjusted to a turbidity equivalent to 0.5 McFarland standard, and inoculated onto the surface of Nutrient Agar (Sigma-Aldrich). Disks containing ciprofloxacin (128 µg/mL), $CuFe_2O_4$-Ag@PANI nanocomposite (128 µg/mL), and a Control were placed on the medium, while a disk with sterile distilled water served as a negative control. The plates were incubated at 37 °C for 24 hours, and the inhibition zones around each disk were measured [9].

II. RESULTS

Characterization of Nanocomposite

The FT-IR spectrum of the $CuFe_2O_4$-Ag@PANI nanocomposite synthesized using flower extract is presented in Fig. 1. It displays two prominent bands at 611 cm^{-1} and 696 cm^{-1}, corresponding to the stretching vibrations of tetrahedral and octahedral metal-oxygen bonds in spinel structures, respectively [10]. Additionally, the FT-IR spectrum reveals a broad band around 3423 cm^{-1}, attributed to the overlapping stretching vibrations of the amine (NH_2) group from algae extract molecules and the O–H stretching of water molecules adsorbed on the surface [11]. The band observed near 1629 cm^{-1} is associated with the stretching vibrations of aromatic C=C bonds [12].

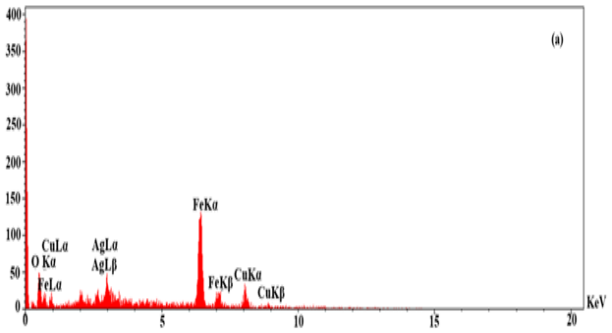

Figure 2 presents the XRD pattern of $CuFe_2O_4$-Ag@PANI. The pattern features characteristic diffraction peaks at 2θ values of 16.89°, 26.94°, 35.33°, 48.51°, 56.12°, 57.3°, and 61.21°, corresponding to the (111), (220), (311), (400), (442), (511), and (440) reflection planes, respectively. These peaks are consistent with the face-centered cubic phase of $CuFe_2O_4$ [13]. Additionally, the peaks at 2θ = 38.18°, 46.32°, 64.75°, and 75.40°, marked with a diamond symbol in Fig.2, correspond to the Bragg reflections of the Ag shell [14]. These findings align with previously reported results [15].

The synthesized sample was analyzed using energy-dispersive X-ray mapping (EDX mapping) to gain deeper insight into the product's elemental composition. Figure 3a confirms the presence of Cu, Fe, Ag, and O atoms, indicating the purity of the $CuFe_2O_4$-Ag@PANI nanocomposite. Additionally, Fig. 3b illustrates the elemental mapping, which reveals the uniform distribution of Cu, Fe, O, and Ag atoms throughout the sample.

The morphology of the synthesized $CuFe_2O_4$-Ag@PANI nanocomposites was examined using field emission scanning electron microscopy

(FESEM). Figures 4a and 4b showcase the uniform distribution of particles and the structural morphology of the $CuFe_2O_4$-Ag@PANI nanocomposites. The size and morphology of the $CuFe_2O_4$-Ag@PANI nanocomposite were analyzed using TEM. The $CuFe_2O_4$-Ag@PANI nanocomposites exhibited a spherical morphology, as shown in Figures 5a and 5b. The average crystalline diameter was approximately 20 nm.

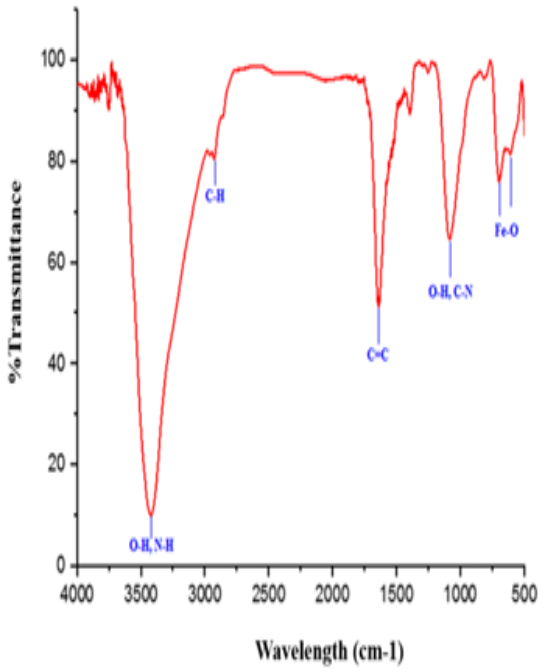

Figure 1 The FT-IR spectrum of $CuFe_2O_4$-Ag@PANI nanocomposite

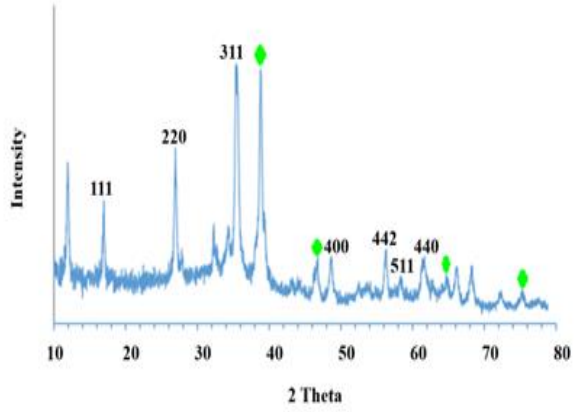

Figure 2 The XRD pattern of synthesized $CuFe_2O_4$-Ag@PANI Nanocomposite.

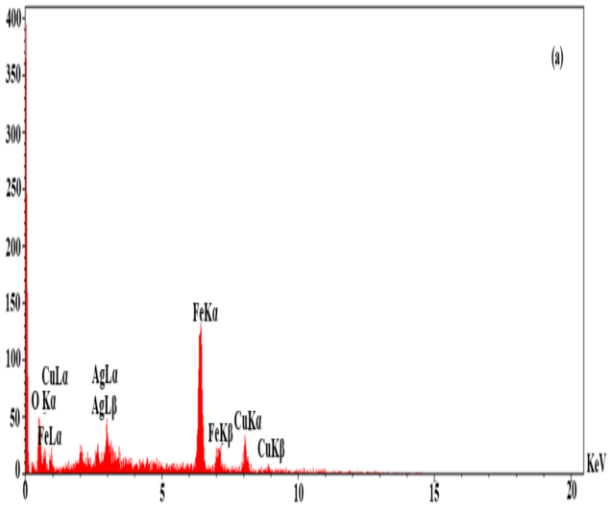

Figure 3 (a) EDX-map image of synthesized $CuFe_2O_4$-Ag@PANI nanocomposite and Figure 3 (b) the elemental mapping, which reveals the uniform distribution of Cu, Fe, O, and Ag atoms throughout the sample

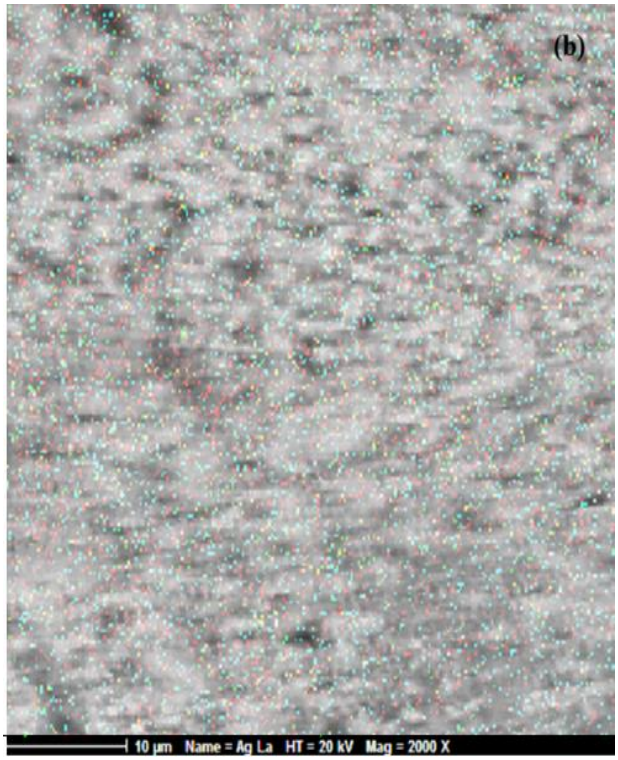

Figure 4 (a) and (b) FESEM image of $CuFe_2O_4$-Ag@PANI nanocomposite

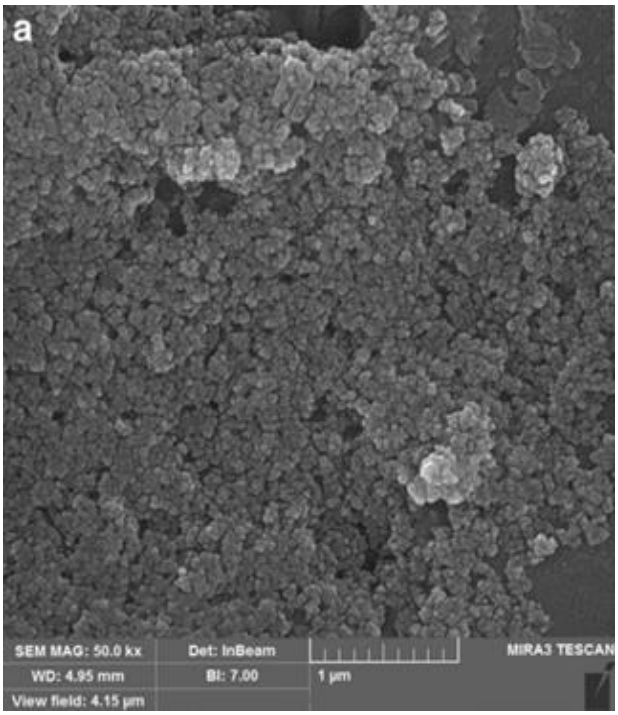

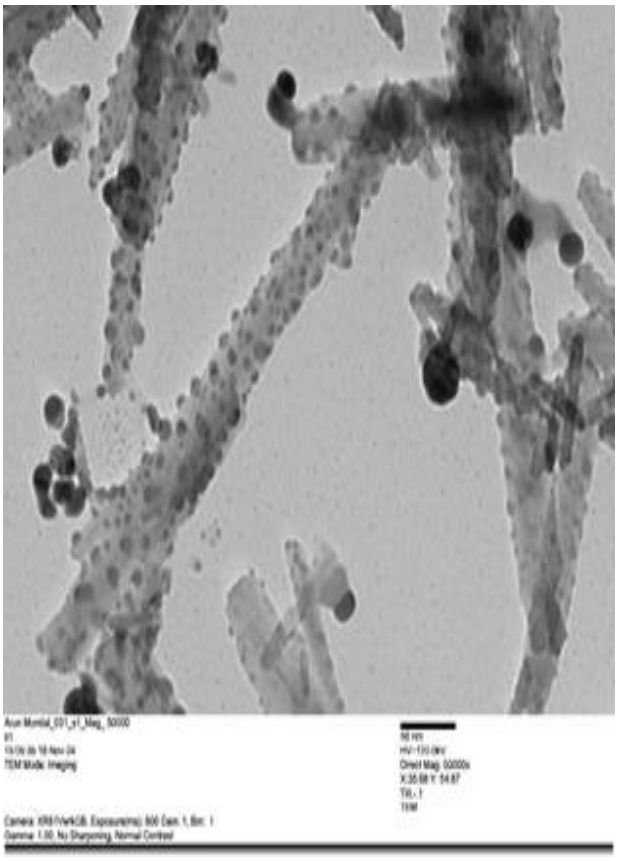

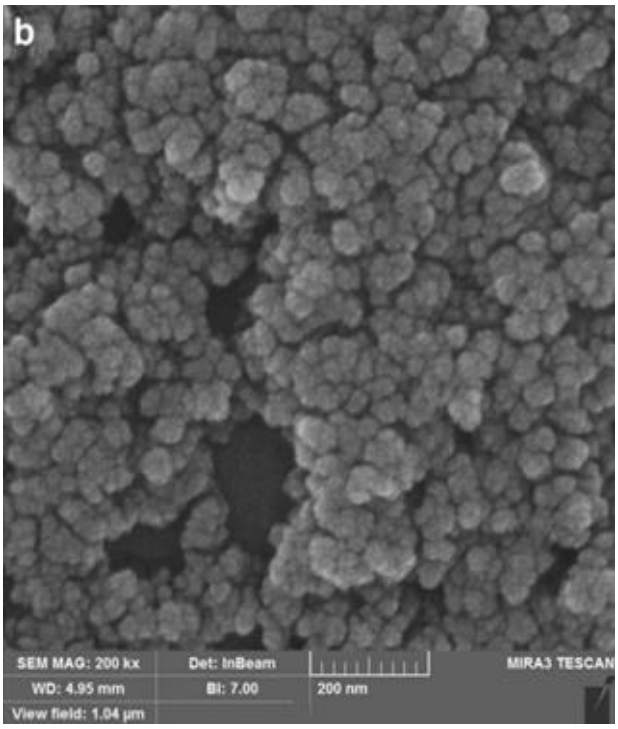

Figure 5 (a) and (b) TEM image of $CuFe_2O_4$-Ag@PANI nanocomposite

Antibacterial Activity of $CuFe_2O_4$-Ag@PANI Nanocomposite

The antibacterial efficacy of the $CuFe_2O_4$-Ag@PANI nanocomposite was evaluated against S. aureus and E. coli (Table 1). The results revealed that the nanocomposite exhibited stronger antibacterial activity against S. aureus (27mm) compared to E. coli (24 mm). Furthermore, the $CuFe_2O_4$-Ag@PANI nanocomposite significantly enhanced the antibacterial activity of the antibiotic, leading to a larger zone of inhibition (ZOI) around the antibiotic disk [16]. The antibacterial activity against S. aureus and E. coli is illustrated in Fig. 6. And Fig. 7 (a) and (b) illustrates the Bacterial plates under the microscop

Table 1 Zone of Inhibition of antibacterial activity against S. aureus and E. coli

Table 1 Zone of Inhibition in mm Against *S. aureus* and *E. coli*

Sample	*S. aureus*	*E. coli*
Control	0	0
Antibiotic (ciprofloxacin)	3.6	3.3
$CuFe_2O_4$	19	15
$CuFe_2O_4$-Ag@PANI nanocomposite	27	24

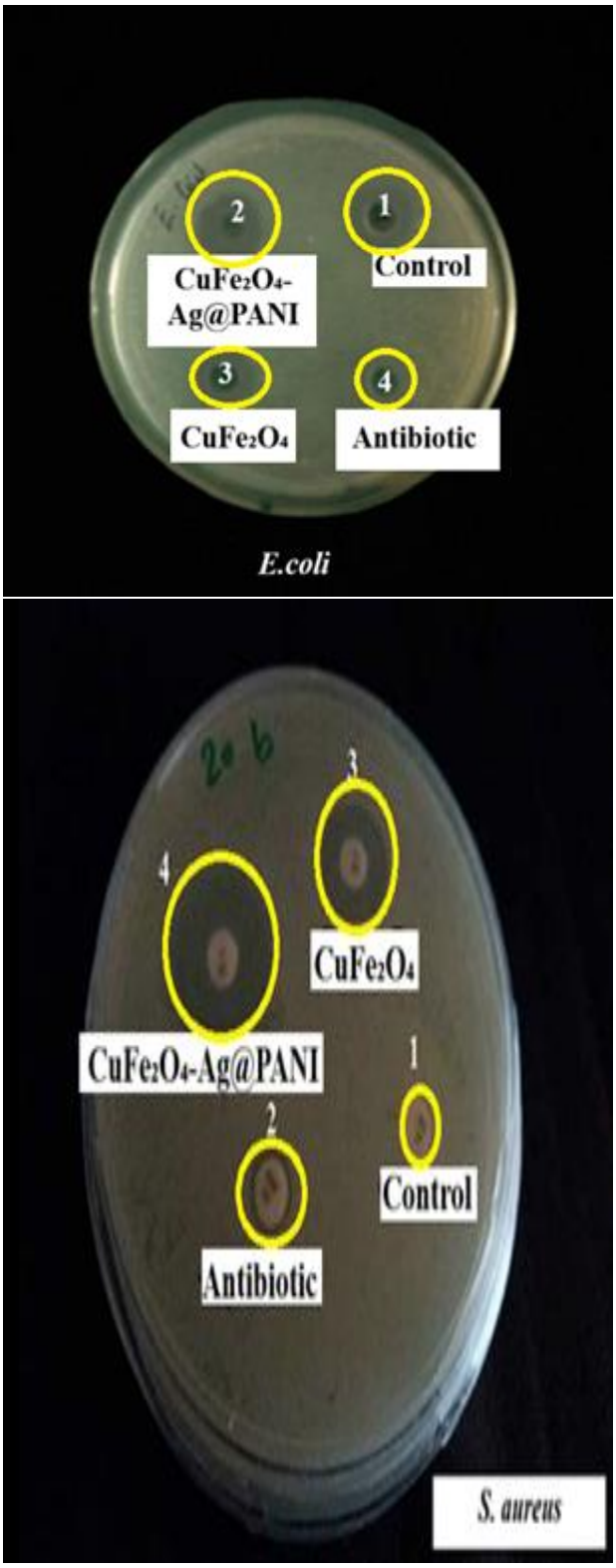

Figure 6 Represents the antibacterial activity against E. coli and S. aureus

S aureus Strain Slide

E. Coli Strain Slide

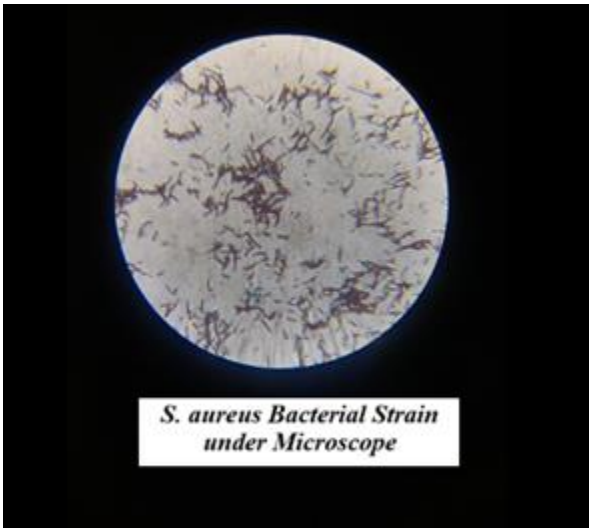

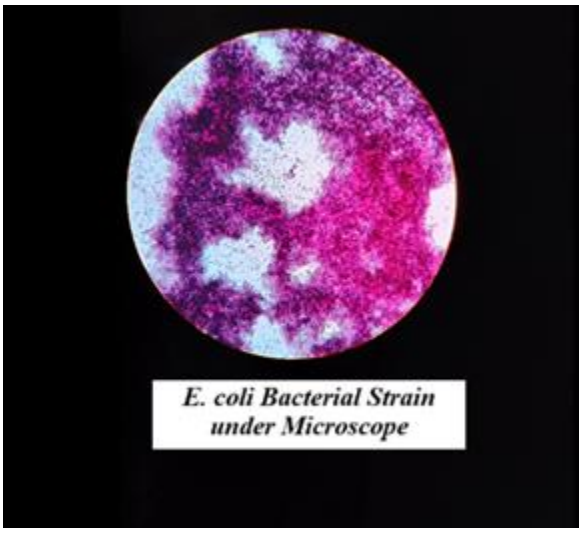

Figure 7 (a) and (b) illustrates the Bacterial Strains Slide

Minimum Inhibitory Concentration (MIC)

The antibacterial potency of the $CuFe_2O_4$-Ag@PANI nanocomposite, the Minimum Inhibitory Concentration (MIC) was determined against Staphylococcus aureus and Escherichia coli. The MIC test helps determine the lowest concentration of an antimicrobial agent required to completely inhibit visible bacterial growth, providing a more precise understanding of its bacteriostatic potential. The MIC values obtained for the $CuFe_2O_4$-Ag@PANI nanocomposite were 62.5 µg/mL against S. aureus and 75 µg/mL against E. coli. These findings are in good agreement with the zone of inhibition results,

where S. aureus (27 mm) showed greater susceptibility than E. coli (24 mm), Table 2. This variation is attributed to the structural differences in bacterial cell walls; Gram-positive S. aureus has a less complex cell wall, making it more vulnerable to the nanocomposite than Gram-negative E. coli.

The MIC test proved highly beneficial in this study as it provided quantitative validation of the composite's antibacterial effect and allowed us to compare its performance with the individual components ($CuFe_2O_4$ and ciprofloxacin). The nanocomposite demonstrated superior activity compared to bare $CuFe_2O_4$ (MIC: 100 µg/mL for S. aureus and 125 µg/mL for E. coli), confirming the synergistic role of Ag and PANI in enhancing antibacterial efficacy. Although ciprofloxacin had the lowest MIC values (1.25 µg/mL for S. aureus, 1.5 µg/mL for E. coli), the $CuFe_2O_4$-Ag@PANI nanocomposite (Figure 8), exhibited significant activity with the added benefit of potential reusability and reduced antibiotic resistance pressure.

Table 2. MIC Values of Various Samples Against S. aureus and E. coli

Sample	MIC Against *S. aureus* (µg/mL)	MIC Against *E. coli* (µg/mL)
Ciprofloxacin	1.25	1.5
$CuFe_2O_4$	100	125
$CuFe_2O_4$-Ag@PANI nanocomposite	62.5	75

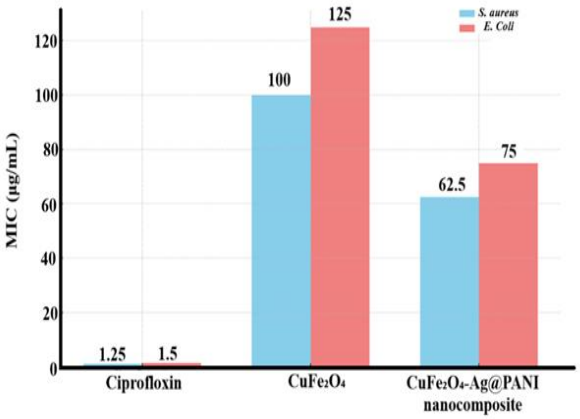

Figure 8 Bar chart showing the MIC values of Ciprofloxacin, $CuFe_2O_4$, and $CuFe_2O_4$-Ag@PANI nanocomposite against S. aureus and E. coli.

Bacteriostatic Rate Analysis

To further evaluate the antibacterial efficiency of the synthesized nanomaterials, the bacteriostatic rate (BR%) was calculated using optical density (OD600) measurements after 24-hour incubation. The BR% was determined using the equation

$BR=((A-B)/A)\times100\%$

where A represents the OD of the control group (bacteria without treatment), and B represents the OD of the treated group. The results revealed significant variation in bacterial growth inhibition across the tested materials in table 3.

Table 3

Sample	BR% (*E. coli*) (%)	BR% (*S. aureus*) (%)
$CuFe_2O_4$	39.1	49
$CuFe_2O_4$-Ag@PANI	60.9	50.5

The antibacterial performance of the synthesized nanocomposite, bacteriostatic rate analysis was conducted based on the measured zones of

inhibition. The $CuFe_2O_4$-Ag@PANI nanocomposite exhibited significantly enhanced antibacterial activity, with a zone of inhibition of 27 mm against S. aureus and 24 mm against E. coli. In comparison, the base material $CuFe_2O_4$ showed only 19 mm and 15 mm zones, respectively.

Bacteriostatic rate analysis revealed that $CuFe_2O_4$-Ag@PANI achieved 60.9% against S. aureus and 50.5 % against E. coli inhibition effectiveness, while $CuFe_2O_4$ alone showed 49.5% effectiveness against S. aureus and 39.1% against E. coli (Figure 9). This substantial improvement confirms the synergistic effect of Ag and PANI, which enhances the membrane disruption capability and reactive oxygen species (ROS) generation. it is evident that $CuFe_2O_4$-Ag@PANI is a superior antibacterial agent, especially against S. aureus, indicating its potential application in developing advanced antibacterial coatings and materials.

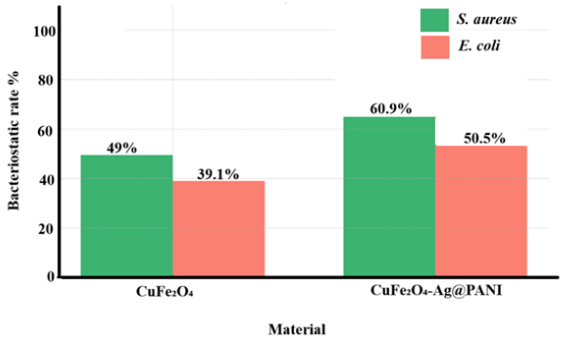

Figure 9 Percentage removal of bacteria (bacteriostatic rate) from different Material

Mechanism of Bacteria

Copper ferrite silver nanocomposites exert a potent antibacterial effect on E. coli by leveraging the combined actions of copper, ferrite, and silver ions. Copper ions disrupt the bacterial cell wall and membrane, cause leakage of cellular contents, and generate reactive oxygen species (ROS), leading to oxidative stress that damages DNA, proteins, and lipids within the bacterial cell. Ferrite enhances the stability and controlled release of copper ions, while silver ions bind to bacterial enzymes, disrupting respiration and reproduction. Silver also promotes ROS production, increasing oxidative stress and causing further damage to cellular components. The synergy between copper and silver ions amplifies these effects, leading to a multi-faceted attack that severely compromises E. coli's cellular integrity, enzyme function, and ability to repair itself, effectively inhibiting bacterial growth and survival.

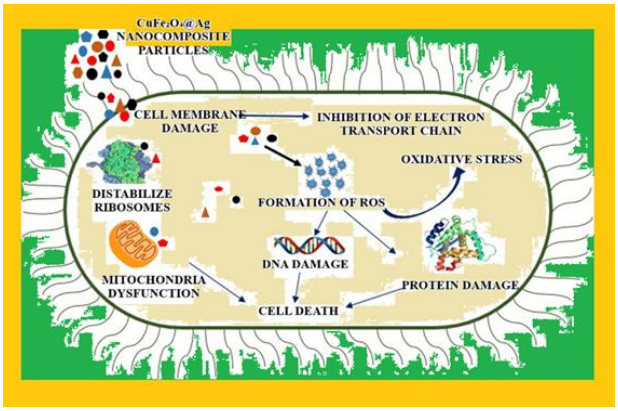

Figure 10 Effect of $CuFe_2O_4$-Ag@PANI nanocomposite on Bacterial mechanism

III. CONCLUSION

The characterization and antibacterial activity of the $CuFe_2O_4$-Ag@PANI nanocomposite synthesized using flower extract were comprehensively analyzed. The FT-IR spectrum revealed distinct bands at 611 cm^{-1} and 696 cm^{-1}, corresponding to the tetrahedral and octahedral metal-oxygen vibrations in the spinel structure, respectively. Additionally, a broad peak at 3423 cm^{-1} indicated the presence of amine (NH_2) groups from algae extract molecules and O–H stretching of adsorbed water, while the band at 1629 cm^{-1} confirmed the presence of aromatic C=C bonds. The XRD pattern further confirmed the crystalline structure of the $CuFe_2O_4$-Ag@PANI nanocomposite, displaying characteristic diffraction peaks at 2θ values of 16.89°, 26.94°, 35.33°, 48.51°, 56.12°, 57.3°, and 61.21°, corresponding to the spinel $CuFe_2O_4$ phase. Additional peaks at 38.18°, 46.32°, 64.75°, and 75.40°, marked with a diamond symbol, were attributed to the Bragg reflections of the Ag shell, confirming the successful incorporation of Ag into the composite structure. Energy-dispersive X-ray (EDX) analysis and elemental mapping confirmed

the presence of Cu, Fe, Ag, and O atoms, indicating the purity of the synthesized nanocomposite and the uniform distribution of its elements. Further morphological analysis using FE-SEM revealed a uniform particle distribution, while TEM imaging confirmed a spherical morphology with an average crystalline size of approximately 20 nm. The antibacterial efficacy of the $CuFe_2O_4$-Ag@PANI nanocomposite was evaluated against S. aureus and E. coli. The results demonstrated significant antibacterial activity, with inhibition zones of 27 mm for S. aureus and 24 mm for E. coli, surpassing that of $CuFe_2O_4$ alone (19 mm and 15 mm, respectively). Moreover, the $CuFe_2O_4$-Ag@PANI nanocomposite enhanced the antibacterial effect of the antibiotic ciprofloxacin, resulting in a larger zone of inhibition (ZOI) around the antibiotic disk. Microscopic imaging further confirmed bacterial growth inhibition, highlighting the nanocomposite's potential as an effective antibacterial agent. In conclusion, the comprehensive characterization results confirm the successful synthesis of $CuFe_2O_4$-Ag@PANI nanocomposite with a well-defined crystalline structure, uniform elemental distribution, and nanoscale spherical morphology. The antibacterial activity assessment through the disk diffusion method revealed substantial inhibition zones for both S. aureus (27 mm) and E. coli (24 mm), which were notably larger than those exhibited by bare $CuFe_2O_4$ (19 mm and 15 mm, respectively). These results were further supported by the Minimum Inhibitory Concentration (MIC) tests, where $CuFe_2O_4$-Ag@PANI exhibited MIC values of 62.5 µg/mL against S. aureus and 75 µg/mL against E. coli, showing improved efficacy compared to $CuFe_2O_4$ alone (100 and 125 µg/mL, respectively). Additionally, the composite enhanced the antibacterial action of ciprofloxacin, indicating its potential for combinatory therapeutic applications. Bacteriostatic rate analysis based on OD600 measurements confirmed the composite's higher antibacterial inhibition, achieving 60.9% for E. coli and 50.5% for S. aureus, while $CuFe_2O_4$ alone showed only 39.1% and 49%, respectively. These findings underscore the synergistic role of Ag and PANI in improving membrane disruption and reactive oxygen species (ROS)-based bacterial killing mechanisms. The ROS and electrostatic interactions caused by the composite were responsible for damaging bacterial membranes, leading to effective inhibition and possible cell death, as illustrated in the proposed mechanistic model. In summary, the $CuFe_2O_4$-Ag@PANI nanocomposite synthesized via a green route exhibits excellent antibacterial properties due to its multi-component synergy, demonstrating promising potential for applications in antibacterial coatings, water purification, and biomedical devices. The study not only highlights the importance of green nanotechnology but also provides a sustainable and effective alternative to conventional antibacterial agents.

REFERENCE

1. Wang, Y., Chen, L., & Li, X. (2023). Emerging trends in antibacterial nanocomposites: A review on synthesis and applications. Nano Research, 16(3), 788-804.
2. Gupta, R., & Sharma, A. (2022). Advances in ferrite nanomaterials: Synthesis, properties, and applications. Materials Today Chemistry, 25, 100973.
3. Singh, P., Das, J., & Roy, P. (2021). Eco-friendly synthesis of nanocomposites for antimicrobial applications: Challenges and future prospects. Environmental Nanotechnology, 14, 101389.
4. Kumar, S., Mehta, P., & Choudhary, N. (2023). Green synthesis of metal nanoparticles using plant extracts: A sustainable approach for biomedical applications. Journal of Nanobiotechnology, 21(1), 56.
5. Zhang, H., Liu, J., & Zhao, R. (2024). Synergistic antibacterial mechanisms of silver-based ferrite nanocomposites. ACS Applied Bio Materials, 7(2), 215-228
6. Wayne, P.A., 2017. CLSI Performance Standards for Antimicrobial Susceptibility Testing. CLSI Document Clinical Laboratory Standards Institute (CLSI): Wayne, PA, USA.
7. Ashraf, I., Agarwal, A., Singh, N.B. and Ray, M.B., 2023. Floral waste synthesized silver nanoparticles as sensor for Cr (VI) ion detection. Environmental Monitoring and Assessment, 195(6), p.671.

8. Shokoofeh, N., Moradi-Shoeili, Z., Naeemi, A.S., Jalali, A., Hedayati, M. and Salehzadeh, A., 2019. Biosynthesis of Fe 3 O 4@ Ag nanocomposite and evaluation of its performance on expression of norA and norB efflux pump genes in ciprofloxacin-resistant Staphylococcus aureus. Biological Trace Element Research, 191, pp.522-530.
9. Pancotti, A., de Barros Souza, M.V., Abreu, A.S., Rezende, S.R., Moreli, M.L., Otero, E.U., Landers, R., Soares, R. and Wang, J., 2024. Evaluation of Antibacterial Activity of Bismuth Ferrites Nanoparticles in the inhibition of E. coli and S. aureus bacteria. Chemistry & Biodiversity, p.e202402048.
10. Truong-Bolduc, Q.C., Hsing, L.C., Villet, R., Bolduc, G.R., Estabrooks, Z., Taguezem, G.F. and Hooper, D.C., 2012. Reduced aeration affects the expression of the NorB efflux pump of Staphylococcus aureus by posttranslational modification of MgrA. Journal of bacteriology, 194(7), pp.1823-1834.
11. Silva, M.D.P., Silva, F.C., Sinfrônio, F.S.M., Paschoal, A.R., Silva, E.N. and Paschoal, C.W.A., 2014. The effect of cobalt substitution in crystal structure and vibrational modes of CuFe2O4 powders obtained by polymeric precursor method. Journal of alloys and compounds, 584, pp.573-580.
12. Buzoglu, L., Maltas, E., Ozmen, M. and Yildiz, S., 2014. Interaction of donepezil with human serum albumin on amine-modified magnetic nanoparticles. Colloids and Surfaces A: Physicochemical and Engineering Aspects, 442, pp.139-145.
13. Shao, W., Liu, X., Min, H., Dong, G., Feng, Q. and Zuo, S., 2015. Preparation, characterization, and antibacterial activity of silver nanoparticle-decorated graphene oxide nanocomposite. ACS applied materials & interfaces, 7(12), pp.6966-6973.
14. Yang, H., Yan, J., Lu, Z., Cheng, X. and Tang, Y., 2009. Photocatalytic activity evaluation of tetragonal CuFe2O4 nanoparticles for the H2 evolution under visible light irradiation. Journal of Alloys and Compounds, 476(1-2), pp.715-719.
15. Sangpour, P., Shabanzadeh, P., Abdollahi, Y. and Zargar, M., 2012. Green biosynthesis of silver nanoparticles using Curcuma longa tuber powder. International journal of nanomedicine, pp.5603-5610.
16. Chaudhary, R., Singh, N.B., Nagpal, G. and Saah, F.K., 2024. Antibacterial activity of reduced graphene-silver oxide nanocomposite against gram-negative bacteria. The Microbe, 5, p.100221.